第 48 卷第 6 期　　硅　酸　盐　学　报　　Vol. 48，No. 6
2020 年 6 月　　JOURNAL OF THE CHINESE CERAMIC SOCIETY　　June，2020
http://www.gxyb.cbpt.cnki.net　　**DOI**：10.14062/j.issn.0454-5648.20190648

A 位阳离子缺位对$(NaBi)_{0.47}Ba_{0.06}TiO_3$无铅压电陶瓷结构和性能的影响

苏春阳，江向平，陈　超，刘俊明，夏　翔，聂　鑫，黄枭坤，庄俊生

(景德镇陶瓷大学材料科学与工程学院，江西省先进陶瓷材料重点实验室，江西 景德镇 333001)

摘　要：采用传统固相法制备 *A* 位阳离子缺位的$(NaBi)_xBa_{0.06}TiO_3$(N_xB_xT–6BT）陶瓷，研究了 Na^+和 Bi^{3+}的缺失对材料结构和压电性能的影响。结果表明：各组分陶瓷样品位于由单斜相(*C*c)和四方相(*P*4bm)构成的准同型相界区域内，随着 Na^+和 Bi^{3+}含量的减少，样品逐渐由单斜相转变为四方相，T_d 明显增加(由 90 ℃增至 160 ℃)，其中 $N_{0.32}B_{0.32}$T–6BT 陶瓷的 d_{33} 在 160 ℃时仍有 23 pC/N，表明 Na^+和 Bi^{3+}的缺失可以明显提高退极化温度，扩大材料的应用范围。

关键词：无铅压电陶瓷；钛酸铋钠；相结构；退极化温度
中图分类号：TQ174　　**文献标志码**：A　　**文章编号**：0454–5648(2020)06–0849–06
网络出版时间：2020–03–24



Impact of Deficiency of *A*-site Cations on Structure and Piezoelectric Properties of Lead-free $(NaBi)_{0.47}Ba_{0.06}TiO_3$ Ceramics

SU Chunyang, *JIANG Xiangping*, *CHEN Chao*, *LIU Junming*, *XIA Xiang*, *NIE Xin*, *HUANG Xiaokun*, *ZHUANG Junsheng*
(Jiangxi Key Laboratory of Advanced Ceramic Materials, Department of Material Science and Engineering, Jingdezhen Ceramic Institute, Jingdezhen 333001, Jiangxi, China)

Abstract: A series of nonstoichiometric $(NaBi)_{0.47}Ba_{0.06}TiO_3$ (NBT–6BT) ceramics were prepared by the conventional solid-state method. The impact of *A*-site nonstoichiometry on the structural and electrical properties of the prepared ceramics was investigated. The room temperature diffraction patterns and Raman spectra revealed the coexistence of the *C*c and *P*4bm phases for all samples. The experimental results in the present work showed that a deficiency in the Bi^{3+} and Na^+ contents could lead to a transformation from the *C*c to *P*4bm phase in addition to a variation in the piezoelectric coefficient d_{33} with the *C*c phase fraction. Favorable thermostability for the piezoelectric properties of the ceramics was observed by testing the depolarization temperature (T_d). Among them, the d_{33} of the $N_{0.32}B_{0.32}$T–6BT ceramics still had a value of 23 pC/N at 160 ℃. These results showed that a deficiency in the Na^+ and Bi^{3+} contents can significantly enhance T_d and extend the temperature region for the application of NBT–6BT ceramics.

Keywords: lead-free ceramic; sodium bismuth titanate; structure; depolarization temperature

1　Introduction

Piezoceramics have been considered essential materials since their widespread application in electromechanical devices, such as actuators, sensors, and transducers[1–4]. Because of their excellent dielectric, piezoelectric and electromechanical coupling coefficients, lead-based materials dominate the commercial market[5]. In view of the harmful effects of lead on the environment, an increasing number of lead-free piezoelectric materials have been studied. Among them, $Na_{0.5}Bi_{0.5}TiO_3$ (NBT) with a high piezoelectric coefficient (d_{33}, about 65 pC/N) is regarded as one of the most promising materials to

收稿日期：2019–09–23。　修订日期：2019–10–27。
基金项目：国家自然科学基金(51562014，51602135，51862016，51762024)；江西省自然科学基金(20171BAB216012)；江西省教育厅科技项目(GJJ170789，GJJ170794，GJJ180718，GJJ170804)。
第一作者：苏春阳(1994—)，男，硕士。
通信作者：江向平(1964—)，男，博士，教授。
陈　超(1983—)，男，博士，副教授。

Received date: 2019–09–23.　**Revised date:** 2019–10–27.
First author: SU Chunyang (1994–), male, Master.
E-mail: 759102764@qq.com
Correspondent author: JIANG Xiangping (1964–), male, Ph.D., Professor.
CHEN Chao (1983–), male, Ph.D., Associate Professor.
E-mail: jiangxp64@163.com
cc2762@163.com

replace Pb(Zr, Ti)O_3 (PZT)-based materials[6–7]. Regrettably, the large coercive field (E_c, about 73 kV/cm), high conductivity during poling and low depolarization temperature (T_d) have restricted its practical application[8]. Therefore, (1–x)($Na_{0.5}Bi_{0.5}$)TiO_3–$x$$BaTiO_3$ (NBT–xBT) solid solution systems have been widely studied in recent years because of their remarkable piezoelectric properties when x=0.06–0.07 for compositions near the morphotropic phase boundary (MPB)[9–11]. However, there are controversies concerning the correlation between the structure and properties in the NBT–xBT system. Takenaka et al. first reported the coexistence of rhombohedral (R3c) and tetragonal (P4bm) phases for NBT–6BT and related it to the enhanced piezoelectric response[12]. Afterwards, Aksel et al. found the monoclinic symmetry (Cc) rather than the R3c space group in NBT with high-resolution powder XRD[13]. Recently, Jiang et al. discovered a Cc+P4bm phase boundary when x=4%–7%[14]. Hence, the structure of NBT–6BT should be further confirmed. Although excellent piezoelectric properties have been found near the MPB, a low depolarization temperature (about 90 ℃) was observed to be a noticeable deficiency for the NBT–xBT system. Different methods have been used to increase the depolarization temperature of the NBT–xBT system. Zhang et al. introduced ZnO into NBT–6BT to form 0–3 type composites to tune the thermal depolarization[15]. Xu et al. used the templated grain growth method to prepare NBT piezoceramics[16]. However, most of the methods were complicated. Guo et al. found that the depolarization temperature changed with an excess of Na^+ and Bi^{3+} in NBT–6BT ceramics[17]. It is evident that the behavior of T_d is strongly related to the mole ratio of Na^+ and Bi^{3+}.

In this paper, we systematically investigated the phase constitution of an unpoled NBT–6BT sample at room temperature. Based on an investigation of the structural evolution of $(NaBi)_{0.47}Ba_{0.06}TiO_3$ samples with changing mole ratios of Na^+ and Bi^{3+}, we also found that a deficiency of Na^+ and Bi^{3+} can enhance T_d significantly. Favorable thermostability was achieved by adjusting the original composition without any doping.

2 Experimental methods

$(NaBi)_xBa_{0.06}TiO_3$ (N_xB_xT–6BT) ceramic samples (with x=0.32, 0.37, 0.42, 0.445 and 0.47) were synthesized by a conventional solid-state method. High-purity powders of Na_2CO_3 (99.8%), Bi_2O_3 (99.99%), $BaCO_3$ (99%) and TiO_2 (99.99%) were used as the raw materials. After mixing by ball milling for 24 h using alcohol as the solvent and ZrO_2 balls as the milling media, the as-mixed powders were dried and calcined at 800 ℃ for 3 h in air as the initial calcination. The obtained powders were reground and then granulated with a 5% (mass fraction) polyvinyl alcohol (PVA) binder. The resultant powders were then granulated and pressed into pellets with a thickness of 1.2 mm and a diameter of 13 mm under a pressure of 18 MPa. Finally, the pressed pellets were sintered in air at 1 150 ℃ for 3 h in a covered alumina crucible.

The crystal structure of the ceramic samples was evaluated using X-ray diffraction (XRD) (D8 Advanced, Bruker axs, Germany). Room temperature Raman spectra were obtained by a Raman spectrometer (LabRAM HR800, Horiba JobinYvon, France). For electrical measurements, silver electrodes were coated on each surface of the sintered pellets and heated at 800 ℃ for 20 min. The ferroelectric hysteresis loops were measured at a frequency of 10 Hz with an automated loop tracer (TF analyzer 2000, aixACCT, Germany). The temperature dependence of the dielectric constant and dielectric loss was measured using an impedance analyzer (4294A, Agilent, USA). The piezoelectric constant of the samples was obtained by a piezo–d_{33} meter (ZJ–3A, China).

3 Results and discussion

The room temperature X-ray diffraction patterns of the unpoled N_xB_xT–6BT (x=0.32, 0.37, 0.42, 0.445 and 0.47) ceramics are shown in Fig. 1. All prepared samples were determined to have a typical perovskite structure. Moreover, it can be seen from Fig. 1(b) that there is a remarkable splitting and broadening in the $\{211\}_{pc}$ and $\{200\}_{pc}$ diffraction peaks, respectively, which indicates that multiphases coexisted and were located at the morphotropic phase boundary (MPB) regions[18]. The broad peaks merged into one sharp peak, implying a phase variation with decreasing contents of Na^+ and Bi^{3+}. Additional analysis with Rietveld refinement is discussed below.

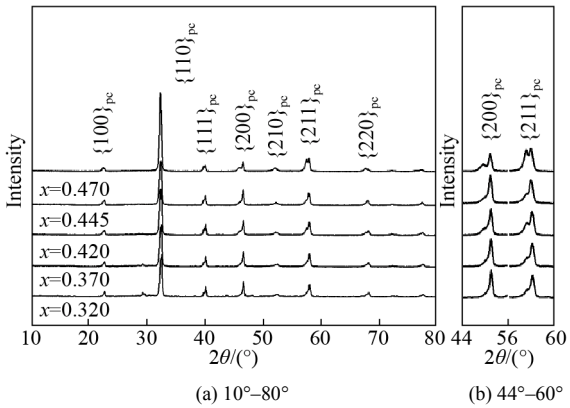


Fig. 1 XRD patterns of the unpoled N_xB_xT–6BT ceramics

Fig. 2 shows the Raman spectra of the N_xB_xT–6BT ceramics at room temperature over the wavenumber range from 150–700 cm^{-1} under the excitation of 532 nm laser sources. It was observed that all obtained

Raman spectra are analogous to other NBT-based ceramics reported previously[19–20]. In general, the Raman bands at 200–400 cm^{-1} are dominated by Ti–O vibrations. The modes at 400–700 cm^{-1} are associated with the vibration of TiO_6-octahedra[20–21]. Therefore, the Raman spectra can be used as a "fingerprint" in identifying the phases involved in the NBT system. With regard to low and high frequencies, the former is linked to the Bi–O band, and the latter is associated with the longitudinal optical (LO) and transverse optical (TO) overlapping bands[22–23]. Hence, modes from 200–700 cm^{-1} were investigated carefully in this study.

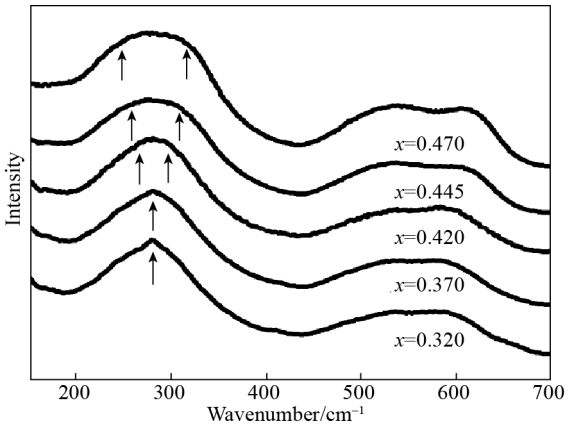


Fig. 2　Room temperature Raman spectra of the N_xB_xT–6BT ceramics

The Raman peak at 260 cm^{-1} gradually merged from two broad peaks into one sharp peak with decreasing Na^+ and Bi^{3+} contents, and the reduced Raman active modes indicated that there was a certain phase change induced by the composition. A similar variation can be found in the 500–600 cm^{-1} bands. According to group theory calculations made by J Kreisel et al., the monoclinic (*C*c) space group has more Raman-active modes than the tetragonal (*P*4bm) group[23]. Therefore, these changes in frequency likely indicate a gradual change from a monoclinic symmetry to tetragonal symmetry with decreasing Na^+ and Bi^{3+} concentrations.

To further investigate the structural change of the N_xB_xT–6BT ceramics, Rietveld refinements of the XRD spectra were carried out using the GSAS package. However, for the pure NBT–6BT (x=0.47), several different space group models of this composition have been reported[12–14]. For the sake of a systematic comparison, the pure NBT–6BT patterns were fitted with different models (*C*c+*R*3c, *C*c+*P*4bm or *R*3c+*P*4bm) and are shown in Fig. 3. After a careful comparison, it was decided that the fitting with the *C*c+*P*4bm model is better than that of the other two–phase space groups.

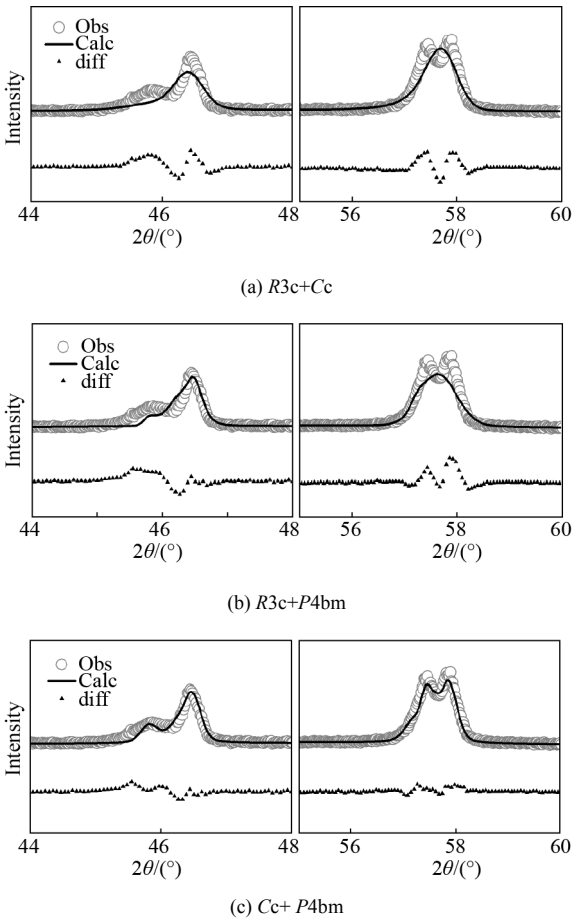
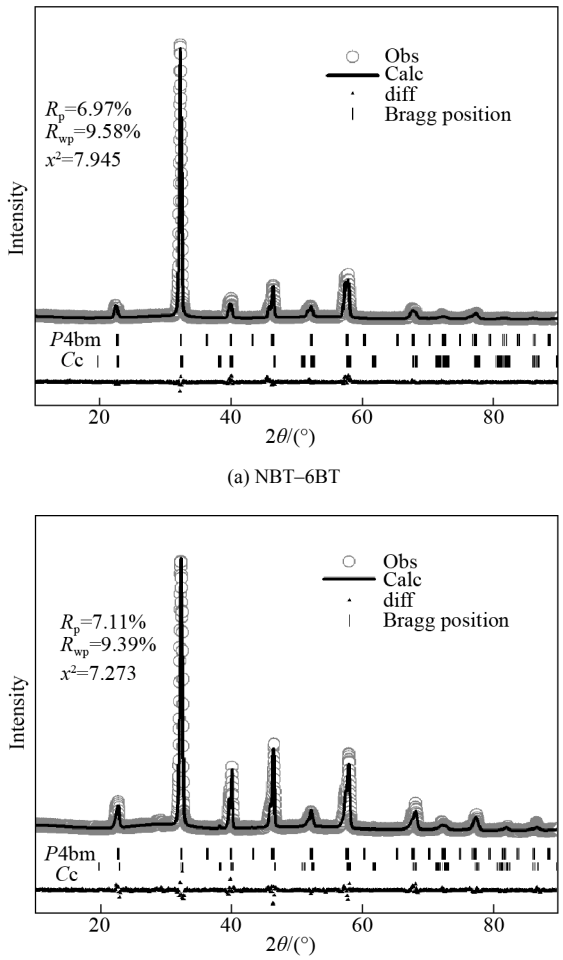


Fig. 3　Rietveld structural refinement plot of the unpoled NBT–6BT ceramic samples

Fig. 4 shows the refinement of the poled samples for the x=0.42 and 0.47 compositions using the *C*c+*P*4bm space group model, and satisfactory refinement results were obtained for all compositions, which corresponds to the viewpoint that these poled compositions have more than one phase coexisting at room temperature. The refined lattice parameters and phase fractions are listed in Table 1. The fraction of the *C*c phase decreases from 65.40% to 38.88% with decreasing Na^+ and Bi^{3+} contents, indicating that a variation in the Na^+ and Bi^{3+} contents can lead to a transformation between the *P*4bm and *C*c phases.

Fig. 5 shows the variation of the P–E hysteresis loops of the prepared ceramics at room temperature with a frequency of 10 Hz. Saturated hysteresis loops are observed for the pure NBT–6BT (x=0.47), and the maximum value of the remnant polarization (P_r) is 35.9 μC/cm^2. Furthermore, the coercive field (E_c) increases and remanent polarization reduces with decreasing Na^+ and Bi^{3+} contents, leading to the appearance of narrow polarization hysteresis loops. This suggests that the decreasing contents of Na^+ and Bi^{3+} results in *A*-site cation vacancies and impedes the sufficient reorientation of ferroelectric domains during electrical poling[24].



(a) NBT–6BT

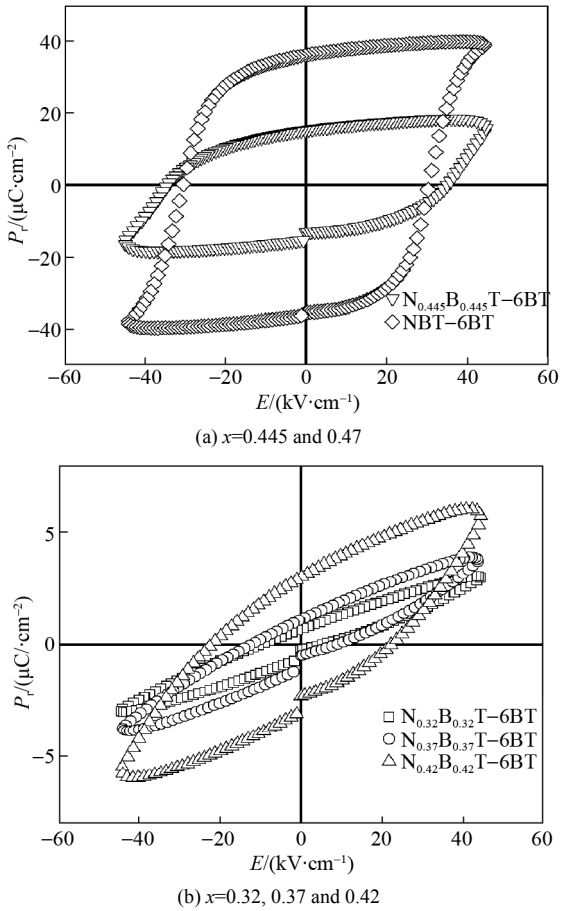
(b) $N_{0.42}B_{0.42}T$–6BT

Fig. 4 Rietveld structural refinement

Table 1 Phase fractions and lattice parameters from the Rietveld structural refinement of the N_xB_xT–6BT sample

x	Phase fraction/%		a/nm	b/nm	c/nm	V/nm^3
0.32	*P*4bm	61.12	0.554	0.554	0.394	0.121
0.32	*C*c	38.88	0.957	0.549	0.554	0.236
0.37	*P*4bm	48.54	0.553	0.553	0.394	0.120
0.37	*C*c	51.46	0.958	0.549	0.554	0.237
0.42	*P*4bm	40.45	0.551	0.551	0.392	0.119
0.42	*C*c	59.55	0.960	0.550	0.555	0.238
0.445	*P*4bm	38.16	0.553	0.553	0.394	0.121
0.445	*C*c	61.84	0.961	0.551	0.555	0.238
0.47	*P*4bm	34.60	0.552	0.552	0.395	0.120
0.47	*C*c	65.40	0.962	0.550	0.557	0.240

To further determine the influence of the deficiency in the Na^+ and Bi^{3+} contents on the piezoelectric properties, the values of the piezoelectric coefficient (d_{33}) and *C*c phase fraction with different compositions were determined and are depicted in Fig. 6 (all the samples were poled at 50 kV/cm for 20 min). The value of d_{33} decreases from 113 to 37 pC/N with decreasing Na^+ and Bi^{3+} contents. Coincidentally, this behavior is consistent with the change in the *C*c phase fraction with x (see Fig. 6). These results indicate that the *C*c phase with low symmetry makes a major contribution to the piezoelectric properties. Similar phenomena were found in other NBT–BT systems[25].



(a) x=0.445 and 0.47

(b) x=0.32, 0.37 and 0.42

Fig. 5 Ferroelectric hysteresis loops of the N_xB_xT–6BT sample at room temperature

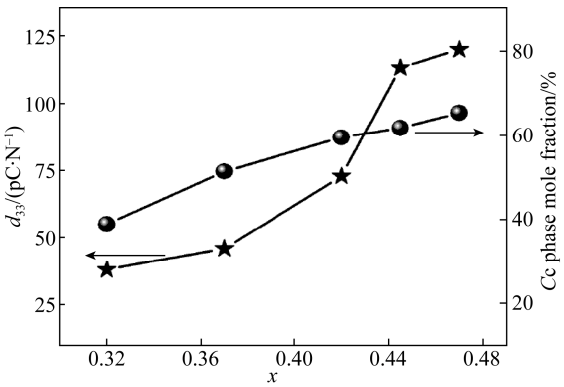


Fig. 6 Piezoelectric coefficient and the fraction of the monoclinic phase in the N_xB_xT–6BT sample

It is generally known that the thermal depolarization temperature which is far below the Curie temperature (T_c), limits the practical application of NBT-based ceramics. The temperature dependence of d_{33} for all compositions is shown in Fig. 7. The

thermostability of the samples is improved by decreasing the Na^+ and Bi^{3+} contents. For the pure NBT–6BT (x=0.47), after exposure to 90 ℃, the retained d_{33} decreases from 113 pC/N to 23 pC/N, which is a decrease of almost 80%. However, there is a negligible variation (from 32 to 31 pC/N) for the $N_{0.32}B_{0.32}T$–6BT ceramics. Particularly, they retain their piezoelectric properties and increase T_d simultaneously when x=0.445 and 0.42. As mentioned above, the decrease in Na^+ and Bi^{3+} results in *A*-site cation vacancies in the ceramics. The clamping effect of the cation vacancies hindered the reorientation of the ferroelectric domains during the heating process.

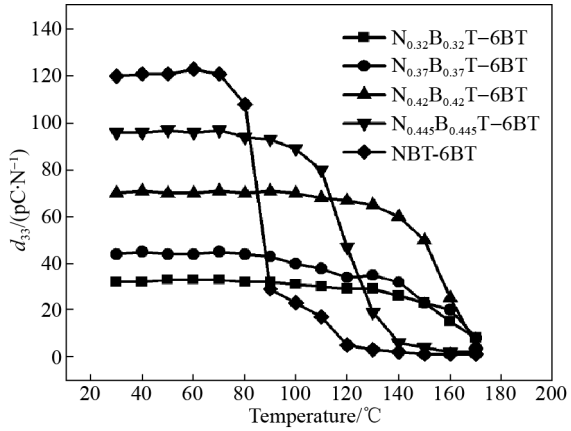


Fig. 7　Temperature dependence of the piezoelectric coefficient for the N_xB_xT–6BT sample

Fig. 8 shows the temperature dependence of the dielectric constant ε_r and dielectric loss tanδ of the N_xB_xT–6BT poled samples with x=0.32, 0.445 and 0.47 at different frequencies. The inflection point of tanδ that is observed at low temperatures is T_d. It can be found that with a decrease in the Na^+ and Bi^{3+} contents, T_d increases, which is in accordance with Fig. 7. The maximum dielectric constant decreases obviously with decreasing Na^+ and Bi^{3+} contents (from 5 898 to 2 442 at 1 MHz). This suggests that *A*-site cation vacancies may induce a change in the conductivity at high temperatures. Moreover, increasing the number of vacancies makes the clamping effect very conspicuous, resulting in an enhancement in T_d. As shown in Fig. 9, vacancies also cause shrinkage of the cell volume. Considering the coexistence of the monoclinic and tetragonal phases, the cell volume can be expressed by the following relation:

$$v = v_C f_C + v_T f_T$$

Where v_C and v_T are the cell volumes of the *C*c and *P*4bm phases, respectively; and f_C and f_T are the phase fractions of the *C*c and *P*4bm phases, respectively.

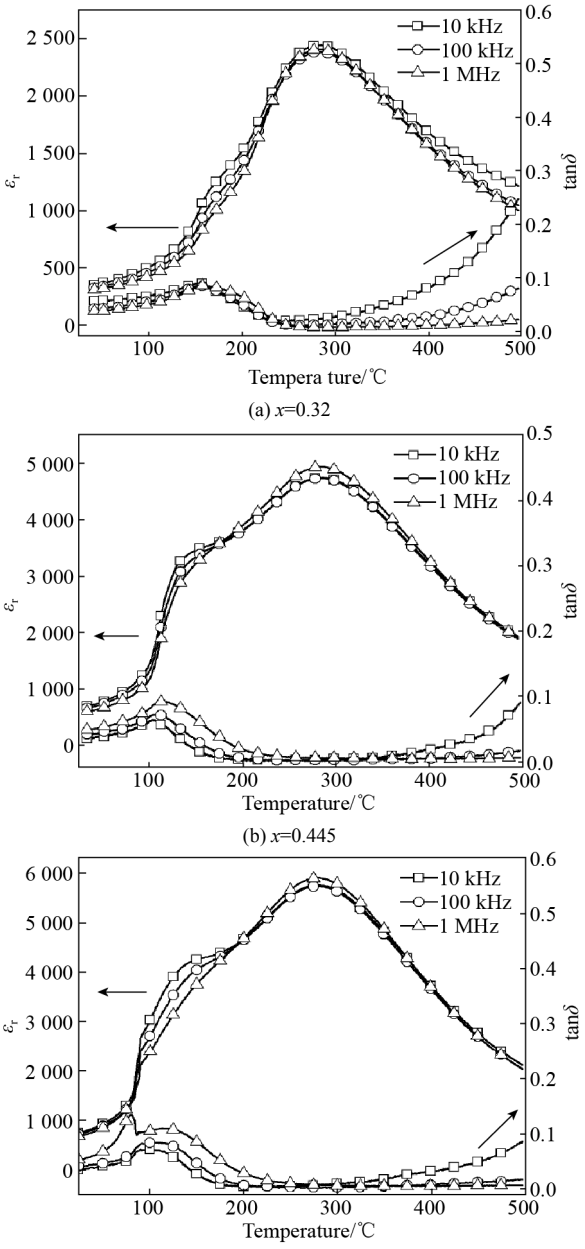


Fig. 8　Temperature dependence of the deielectric constant ε_r and deielectric loss tanδ of poled N_xB_xT–6BT samples with x=0.32,0.445 and 0.47

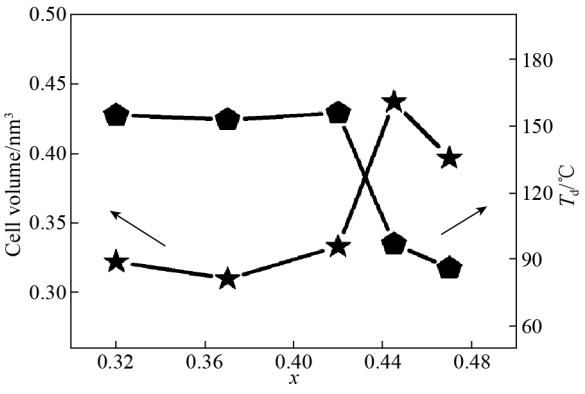


Fig. 9　Cell volume and composition dependence of T_d for the N_xB_xT–6BT samples

4 Conclusions

$Na_xBi_xBa_{0.06}TiO_3$ ceramic samples were successfully synthesized by a conventional solid-state method. XRD and Raman results confirmed the existence of a morphotropic phase boundary. According to the XRD Rietveld refinements, the coexistence of the *C*c and *P*4bm phases at room temperature for $0.32 \leqslant x \leqslant 0.47$ was observed. With a decrease in Na^+ and Bi^{3+} contents, the fraction of the *C*c phase declined from 65.40% to 38.88%. On the other hand, the T_d and T_m (the temperature where ε_r reaches a maximum) values obviously increased with a deficiency in Na^+ and Bi^{3+} contents. The d_{33} of the $N_{0.32}B_{0.32}T$–6BT ceramics remained at 23 pC/N at 160 ℃, which means that a decrease in the Na^+ and Bi^{3+} contents can significantly enhance T_d and extend the temperature range for practical applications.

References:

[1] LI J F, WANG K, ZHU F Y, et al. (K,Na)NbO_3–based lead-free piezoceramics: fundamental aspects, processing technologies, and remaining challenges[J]. J Am Ceram Soc, 2013, 96(12): 3677–96.

[2] RöDEL J, JO W, SEIFERT K T P, et al. Perspective on the development of lead-free piezoceramics[J]. J Am Ceram Soc, 2009, 92(6): 1153–77.

[3] MCQUADE R R, DOLGOS M R. A review of the structure-property relationships in lead-free piezoelectric (1–*x*)$Na_{0.5}Bi_{0.5}TiO_3$–(*x*)$BaTiO_3$[J]. J Solid State Chem, 2016, 242: 140–147.

[4] SHVARTSMAN V V, LUPASCU D C, GREEN D J. Lead-free relaxor ferroelectrics[J]. J Am Ceram Soc, 2012, 95(1): 1–26.

[5] RODEL J, Webber K G, Dittmer R, et al. Transferring lead-free piezoelectric ceramics into application[J]. J Eur Ceram Soc, 2015, 35(6): 1659–1681.

[6] CHENG R, XU Z. Structure and electrical properties of $Bi_{1/2}Na_{1/2}TiO_3$-based lead-free piezoelectric ceramics[J]. RSC Adv, 2015, 5(52): 41646–41652.

[7] WU M, LU Y, LI Y. Structural and electrical properties of Er_2O_3-doped $Na_{1/2}Bi_{1/2}TiO_3$ lead-free piezoceramics[J]. J Am Ceram Soc, 2007, 90(11): 3642–3645.

[8] SASIKUMAR S, SARAVANAN R, SARAVANAKUMAR S, et al. Charge correlation of ferroelectric and piezoelectric properties of (1–*x*)$(Na_{0.5}Bi_{0.5})TiO_3$–*x*$BaTiO_3$ lead-free ceramic solid solution[J]. J Mater Sci, 2017, 28(13): 9950–9963.

[9] JIANG X P, LI L Z, CHEN C, et al. Dielectric properties of Mn-doped $(Na_{0.8}K_{0.2})_{0.5}Bi_{0.5}TiO_3$ ceramics[J]. Mater Lett, 2006, 60(15): 1786–1790.

[10] ZHENG L, YI X, ZHANG S, et al. Complete set of material constants of 0.95$(Na_{0.5}Bi_{0.5})TiO_3$–0.05$BaTiO_3$ lead-free piezoelectric single crystal and the delineation of extrinsic contributions[J]. Appl Phys Lett, 2013, 103(12): 122905(1–4).

[11] RAO B N, AVDEEV M, KENNEDY B, et al. Phase boundary at x = 0.03 and its anomalous influence on the structure and properties in the lead-free piezoelectric (1–*x*)$Na_{1/2}Bi_{1/2}TiO_3$–(*x*)$BaTiO_3$[J]. Phys Rev B, 2015, 92 (21): 214107(1–11).

[12] TAKENAKA T, MARUYAMA K, SAKATA K. $(Bi_{1/2}Na_{1/2})TiO_3$–$BaTiO_3$ system for lead-free piezoelectric ceramics[J]. Jpn J Appl Phys, 1991, 30(9S): 2236–2239.

[13] AKSEL E, FORRESTER J S, KOWALSKI B, et al. Phase transition sequence in sodium bismuth titanate observed using high-resolution *x*-ray diffraction[J]. Appl Phys Lett, 2011, 99(22): 2651(1–3).

[14] XIA X, JIANG X, CHEN C, et al. Composition and poling-induced modulation on photoluminescence properties for NBT–*x*BT: Pr^{3+} ceramics[J]. J Eur Ceram Soc, 2017, 38(4): 1498–1507.

[15] ZHANG J, PAN Z, GUO F F, et al. Semiconductor/relaxor 0–3 type composites without thermal depolarization in $Bi_{0.5}Na_{0.5}TiO_3$–based lead-free piezoceramics[J]. NAT COMMUN, 2015, 6: 1–10.

[16] ZHANG H, XU P, PATTERSON E, et al. Preparation and enhanced electrical properties of grain-oriented $(Bi_{1/2}Na_{1/2})TiO_3$-based lead-free incipient piezoceramics[J]. J Eur Ceram Soc, 2015, 35(9): 2501–2512.

[17] GUO Y, GU M, LUO H, et al. Composition-induced antiferroelectric phase and giant strain in lead-free $(Na_y,Bi_z)Ti_{1-x}O_{3(1-x)}$–*x*$BaTiO_3$ ceramics. Phys Rev B. 2011, 83(5): 3002–3005.

[18] SWAIN S, KUMAR K S, KUMAR P. Dielectric, optical, piezoelectric and ferroelectric studies of NBT–BT ceramics near MPB[J]. Ceram Int, 2015, 41(9): 10710–10717.

[19] WYLIE–VAN E, DAMJANOVIC D, KLEIN N, et al. Structural complexity of $(Na_{0.5}Bi_{0.5})TiO_3$–$BaTiO_3$ as revealed by Raman spectroscopy[J]. Phys Rev B, 2010, 82(10): 104112(1–7).

[20] CHEN C, ZHANG H, DENG H, et al. Electric field and temperature-induced phase transition in Mn-doped $Na_{1/2}Bi_{1/2}TiO_3$–5.0% $BaTiO_3$ single crystals investigated by micro-Raman scattering[J]. Appl Phys Lett, 2014, 104(14): 142902(1–5).

[21] AKSEL E, FORRESTER J S, KOWALSKI B, et al. Structure and properties of Fe-modified $Na_{0.5}Bi_{0.5}TiO_3$ at ambient and elevated temperature[J]. Phys Rev B, 2012, 85(2): 024121(1–11).

[22] ROUT D, MOON K S, KANG S J L, et al. Dielectric and Raman scattering studies of phase transitions in the (100–*x*)$Na_{0.5}Bi_{0.5}TiO_3$–*x*$SrTiO_3$ system[J]. J Appl Phys, 2010, 108(8): 809(1–7).

[23] KREISEL J, GLAZER A M, JONES G, et al. An *x*-ray, diffraction and Raman spectroscopy investigation of *A*-site, substituted perovskite compounds: the $(Na_{1-x}K_x)_{0.5}Bi_{0.5}TiO_3$ ($0<x<1$) solid solution[J]. J PHYS–CONDENS MAT, 2000, 12(12): 3267–3280.

[24] MA C, TAN X, DUL'KIN E, et al. Domain structure-dielectric property relationship in lead-free (1−*x*)$(Bi_{1/2}Na_{1/2})TiO_3$*x*$BaTiO_3$ ceramics[J]. J Appl Phys, 2010, 108(10): 104105(1–8).

[25] RAO B N, FITCH A N, RANJAN R N. Ferroelectric-ferroelectric phase coexistence in $Na_{1/2}Bi_{1/2}TiO_3$[J]. Phys Rev B, 2013, 87(6): 173–177.